Advances in Environmental Technology 4 (2018) 223-231

Advances in Environmental Technology

journal homepage: http://aet.irost.ir

Efficient removal of Ag^+ and Cu^{2+} using imine-modified/mesoporous silica-coated magnetic nanoparticles

Hadis Shooshtary[a], Leila Hajiaghababaei[a,*], Alireza Badiei[b], Mohammad Reza Ganjali[c], Ghodsi Mohammadi Ziarani[d]

[a] *Department of Chemistry, Yadegar-e-Imam Khomeini (RAH) Shahre Rey Branch, Islamic Azad University, Tehran, Iran*

[b] *School of Chemistry, College of Science, University of Tehran, Tehran, Iran*

[c] *Center of Excellence in Electrochemistry, School of Chemistry, College of Science, University of Tehran, Tehran, Iran*

[d] *Department of Chemistry, Alzahra University, Tehran, Iran*

ARTICLE INFO

Article history:
Received 1 December 2018
Received in revised form
9 August 2019
Accepted 24 August 2019

Keywords:
Ag^+
Cu^{2+}
Imine-modified silica-coated magnetic nanoparticles
Removal
Wastewater

ABSTRACT

The present work focuses on the synthesis and application of imine-modified silica-coated magnetic (IM-SCM) nanoparticles. The X-ray diffraction (XRD) tests indicated the presence of highly crystalline cubic spinel magnetite both before and after coating with the silica. The FTIR spectra also proved the successful surface coating and imine-modification of the Fe_3O_4 nanoparticles. Further investigations were performed to examine the capability of the modified IM-SCM nanoparticles for simultaneous removal of Ag^+ and Cu^{2+} from the water samples. Atomic absorption spectrometry was used for ion determination. The best operating conditions for removing the target ions were a pH=5-9 and a stirring time=30 min. Only 20 mL of 3M nitric acid was used for stripping the ions using the IM-SCM nanoparticles. The resulting data were found to fit well with the Langmuir model, and the maximum capacity of the adsorbent was determined to be 270.3 (± 1.4) mg and 256.4 (± 0.9) mg of Ag^+ and Cu^{2+} /g of IM-SCM, respectively. The adsorbent was successfully used for simultaneously removing the target ions from the wastewater samples.

1. Introduction

Finding the appropriate adsorbents is the key to maximizing adsorption efficiency. Metal and metal oxide nanoparticles have long been used for treating water and wastewater samples; they have been found to enjoy advantages such as a large surface area to volume ratio, affectivity at low concentrations, ease of separation, regeneration and reusability, etc. over conventional adsorbents [1]. Recently, many researchers have been attracted to the area of magnetic adsorbents [2-6]. On the other hand, mesoporous silica materials are very interesting materials. They have a high specific surface area, limited pore size distribution range, and high surface concentration of –OH groups that can be easily modified at their silanol groups through grafting with commercial organosilane compounds. The compounds are also advantageous for use in aqueous solutions since they have a hydrophobic surface. Various mesoporous materials have been reportedly used in adsorption applications such as the elimination and preconcentration of metal ions [7-14], organic compounds [15], dyes [16-18], radio nuclides [19] and anionic species [20,21]. The rather recent advent and application of hybrid sorbents has created new opportunities in various fields [3,4,22-24]. The function of such materials are based on the combination of two or more removal mechanisms, e.g., physical adsorption, electrostatic, ion-exchange, and hard/soft acid-base interactions [25]. In this light, preparing the sorbents by combining magnetic nanoparticles and functionalized mesoporous silica appears to have the potential to produce valuable results. In this study, the nanoparticles of Fe_3O_4 were prepared and coated with mesoporous silica. Next, they were modified with imine

*Corresponding author. Tel.: +989125017614
E-mail address: lhajiaghababaei@yahoo.com
DOI: 10.22104/aet.2019.3324.1164

(Figure 1); this novel sorbent was used to simultaneous remove Ag^{+} and Cu^{2+} ions from water solutions.

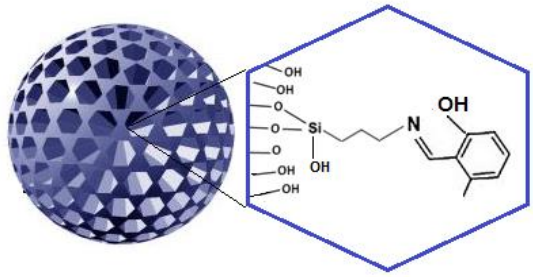

Fig. 1. Structure of Imine functionalized silica-coated Fe_3O_4 magnetic nanoparticles.

2. Materials and methods

2.1. Reagents

The $FeCl_2.4H_2O$, 98%, $FeCl_3.6H_2O$, 98%, absolute ethanol, glycerol, 99% and 25% aqueous solution of ammonium were all obtained from Merck. All solvents (Merck) were used without additional purification. The analytical grade nitrate salts of sodium, manganese, magnesium, cobalt, silver, nickel, zinc, cadmium, lead, chromium and copper (all from Merck) were of the highest purity available and used without further purification. The tetraethyl orthosilicate (TEOS), 98%, 3-amino propyltrimethoxysilane (APTES), 97%, and 2-hydroxybenzaldehyde, 99%, were supplied by Sigma-Aldrich. Distilled deionized water (DDIW) was used in all the experiments. The 1000 mg/L solutions of all metal ions were prepared by dissolving the appropriate amounts of the corresponding nitrate salts in the DDIW and used as the stock solutions for preparing the rest of the solutions through dilution.

2.2. Instruments

The FT-IR spectra were acquired in the range of 400-4000 cm^{-1} on a RAYLEIGH WQF-510A FT-IR spectrophotometer, and the samples were prepared through the KBr pellet technique. XRD analysis was used to determine the crystal structures of the products using a X'Pert Pro MPD diffractometer equipped with a Cu-K_α radiation source (λ= 1.5418 Å) at 40 kV and 40 mA. The pH of all the solutions were monitored using a Jenway3520 pH-meter and a combined glass-calomel electrode. An UP 400S Hielscher ultrasonic probe with an operating voltage of 450 V was used to disperse the nanoparticles in the solution, and a 1.4 T strong magnet (5 cm×5 cm×4 cm) was applied for magnetic materials separation.The atomic absorption analyses were run on a PG-990 flame atomic absorption spectrometer using hollow cathode lamps and an air/acetylene burner at a slit width of 0.4 nm, lamp current of 5.0 mA, and respective wavelengths of 328.1 nm and 324.7 nm for Ag^{+} and Cu^{2+}.

2.3. Synthesis of IM-SCM nano-particles

2.3.1. Magnetite nanoparticles (M-NPs)

The magnetic nanoparticles (M-NPs) were prepared as described in [23] with minor alterations. The typical procedure involved dissolving 4.30 and 11.68 g of $FeCl_2.4H_2O$ and $FeCl_3.6H_2O$ in 200 mL DDIW in a nitrogen atmosphere under vigorous stirring at 90 ºC. Next, 25 mL of 25% aqueous ammonia was added to the solution, immediately changing the color of the solution from orange to black; the produced M-NPs were separated. Then, they were repeatedly washed with DDIW and rinsed with a 0.02 mol/L NaCl solution. Finally, the M-NPs were dispersed into and stored in DDIW at a concentration of about 40 g/L.

2.3.2. Silica-coated magnetic nanoparticles (SCM-NPs)

The SCM nanoparticles were prepared as reported in [4]. The procedure involved transferring 20 mL of the M-NPs suspension described above into a round-bottom flask and allowing the solid particles to settle so as to remove the supernatant. Next, an 80 mL of a 10% v/v aqueous solution of tetraethyl orthosilicate (TEOS) was added to the flask, and this was followed by adding 60 mL of glycerol. The pH of this mixture was set at 4.6 using acetic acid, and the mixture was stirred-heated at 90 °C for 120 min in a nitrogen atmosphere. Then, the mixture was cooled to ambient temperature, and the solid content was repeatedly washed with methanol and DDIW (5 × 200 mL); then it was stored in DDIW at 40 g/L.

2.3.3. Amine-modified silica-coated magnetite nanoparticles (ASCM-NPs)

The nanoparticles were modified as previously reported [3]. It involved dispersing 1g of SCM-NPs in 100 mL of ethanol under sonication, which was followed by adding a solution of (3-aminopropyl) trimethoxysilane (APTES, 3.5 mmol, 10% in 10 mL ethanol) and refluxing under an N_2 atmosphere. The resulting solid particles were separated using a magnet, repeatedly washed with ethanol, and vacuum dried at 60 °C.

2.3.4. Imine-modified silica-coated magnetic nanoparticles (IM-SCM NPs)

To this end, 1g of the ASCM-NPs was dispersed in 50 mL of absolute ethanol by sonication. Subsequently, a solution of 3.5 mmol of salicylaldehyde in 50 mL of absolute ethanol was added to this mixture and stirred for one day at ambient temperature; then, it was refluxed for another 12 h. The resulting product was washed with sequentially dichloromethane, methanol, and chloroform before drying at 60 °C under a vacuum.

2.4. Extraction experiments

The extraction procedure using the IM-SCM NPs involved adding desirable amounts (e.g. 20 mg) of the adsorbent to

a volume of 3 mg/L solution of the target ions and stirring it for at least 30 min. Then, the resulting mixture was filtrated using filter paper; the ions were stripped through washing with 20 mL of a 3.0 mol/L solution of nitric acid and analyzed via flame atomic absorption spectroscopy.

2.5. Equilibrium Evaluations

Adsorption isotherms are used to determine the profile of equilibrium solute concentration Ce (mg/L) versus the mass of the solute adsorbed per that of the adsorbent qe (mg/g). In the present work, the Freundlich, Langmuir, and Temkin isotherm models were used. The Freundlich model is based on assuming a heterogeneous surface and a non-uniform distribution of heat of adsorption over it, while the Langmuir model basically assumes the sorption to take place at specific homogeneous sites of the adsorbent.
The linearized Langmuir model is given below [26]:

$$C_e / q_e = 1/b\ q_m + C_e / q \quad (1)$$

where q_m and b are the maximum adsorption capacity observed in the case of complete monolayer coverage and the equilibrium constant (L/mg), respectively.

$$\text{Log } q_e = \log K_f + \frac{1}{nf} \log C_e \quad (2)$$

As to the Freundlich model, the linearized equation is where K_f and $1/n_f$ are a rough indicator of the adsorption capacity and the adsorption intensity, respectively. $1/n_f < 1$ indicates a normal adsorption. The value gets closer to zero in more heterogeneous cases. If $n_f = 1$, then the partition between the two phases are independent of the concentration and $1/n_f > 1$ indicates cooperative adsorption. On the other hand, the Temkin isotherm model is commonly used in the case of heterogeneous surface energy systems, in which the distribution of sorption heat is not homogeneous [28]; its linearized form is:

$$q_e = B\ \text{Ln}\ k_t + B\ \text{Ln}\ C_e \quad (3)$$

where B = RT/b is a constant which is a function of the heat of sorption (J/mol) and determined from the Temkin plots (qe vs. ln Ce); b and R are the Temkin isotherm constant and universal gas constant (8.314 J/mol. K), respectively; T shows the temperature (K); and K_t is the equilibrium binding constant of the isotherm (L/g). Different solutions of the target ions, with concentrations in the range of 100-1000 mg/L at pH=5, were prepared to obtain the adsorption isotherm data. Then, 20 mg of adsorbent was added to each solution and stirred for 30 min. The resulting mixtures were filtrated and analyzed through flame atomic absorption spectroscopy.

2.6. Standard addition calibration

The standard additions method is a calibration method which is appropriate for measurement in a complex matrix such as wastewater samples. A typical procedure involves preparing several solutions containing the same amount of unknown but different amounts of standard. In this study, four 50 mL volumetric flasks were each filled with 10 mL of the wastewater samples. Then the standard was added in differing amounts (0, 2, 3, and 4 mL of 50 mg/L). The flasks were then diluted to the mark and mixed well. After measuring the response for all of the solutions, the changes of absorption versus the standard concentration were plotted. A simple linear least squares analysis was made using the slope and intercept functions of Microsoft Excel. To find the original concentration of the unknown, the value of X at y=0 from y= mX+b was calculated.

3. Results and discussion

3.1. Characterizing the adsorbent

The FTIR spectra obtained for the modified and unmodified SCM-NPs (Figure 2) offer meaningful information about the bonding sites of the samples. It is worthy to note that the glitches at 2400 cm^{-1} reflect the stretching vibration of the CO_2 originating from the air inside the sample chamber. The strong, broad signals at 455 cm^{-1} and 562 cm^{-1} that are observed in the case of the modified and unmodified Fe_3O_4 reflect the stretching vibrations of the Fe–O bonds. The band observed at 3382 cm^{-1} in cases originates from the O–H group, while those at 808, 947, 1089 and 1214 cm^{-1} reflect the stretching of Si–OH and Si–O–Si and are observed in the spectra of the silica-coated samples. Comparing the FT-IR spectra of the SCM-NPs, ASCM-NPs and IM-SCM NPs, the characteristic bands are at 2800—2950 cm^{-1} and 1450 cm^{-1}, which is typical of the $–CH_2$ vibration of the APTES groups.

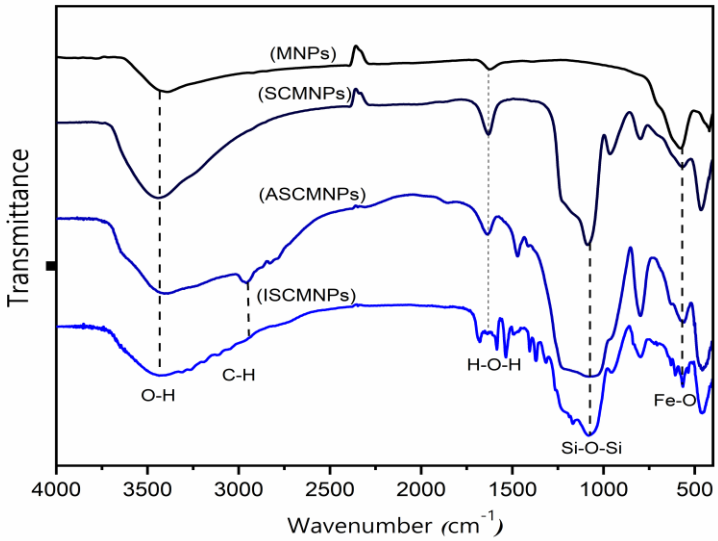

Fig. 2. FT-IR spectra of M-NPs, SCM-NPs, ASCM-NPs and IM-SCM NPs.

The structures and compositions of the M-NPs and IM-SCM NPs were rechecked using PXRD. The result obtained for the M-NP is found in 10 ≦ 2Theta≦ 80°, Figure 3, and shows all lines of magnetite (JCPDS No. 19-0629) with intensities matching the theoretical values. Still, the lattice parameter is a little on the small side: a=8.372(3) Å.

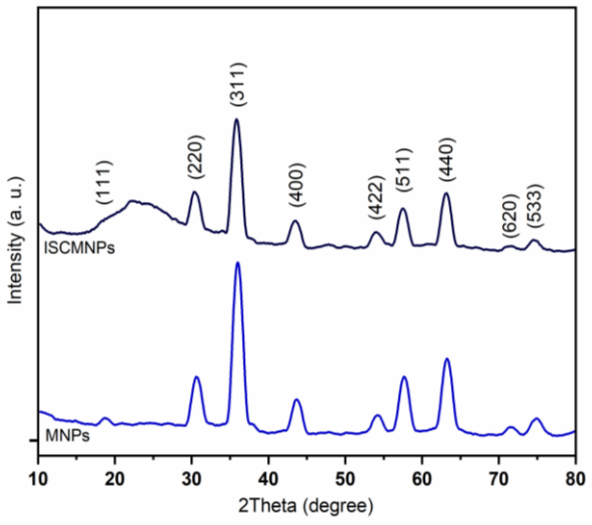

Fig. 3. X-ray diffraction patterns of M-NPs, IM-SCM NPs.

No trace of anisotropic line broadening is present and, hence, NPs can be concluded as sphere-like particles with diameters of 8.1 nm based on the Scherrer equation. The wide reflection at 2θ = 23.1° in the case of SCM-NPs (Figure 3) is due to the amorphous silica (JCPDS No. 29-0085), indicating the coating of the magnetite cores with silica. A scanning electron microscope (SEM) is quite useful for characterizing the morphological structure and size of the magnetite nanoparticles. The SEM image of the prepared nanomaterials is shown in Figure 4 and clearly show that the synthesized nanoparticles are spheroidal in shape. As shown in the figure, the diameter of the particles is about 45-55 nm.

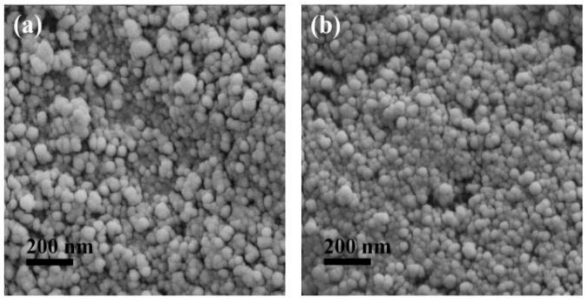

Fig. 4. SEM images of a: IM-SCM NPs and b: SCM NPs samples.

To obtain more direct information on the size and morphology of the particles, the transmission electron microscopy (TEM) micrographs of the obtained nanoparticles were investigated (Figure 5). The TEM analysis of the nanoparticles indicated spherical morphologies. According to the TEM images, the mean particle size was about 45 nm.

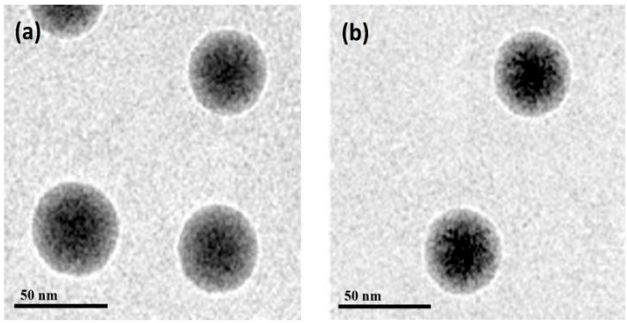

Fig. 5. TEM images of a: IM-SCM NPs and b: SCM NPs samples.

Magnetic hysteresis loops of all the samples were investigated at room temperature via vibrating sample magnetometry (VSM) to study the magnetic properties of the produced mesoporous nanospheres. Figure 6 shows the magnetization curves of all the synthesized materials. The saturation magnetization values (Ms) observed for a: magnetic nanoparticles, b: silica-coated magnetic nanoparticles, and c: modified magnetic silica-coated nanoparticles were found to be 62, 47, and 21 emu/g, respectively. The decrease in the magnetic saturation of the Fe_3O_4 based core-shell nanospheres compared to the naked Fe_3O_4 nanoparticles could be attributed to the presence of the coated SiO_2, mesoporous materials and organosilanes. However, these synthesized functional magnetic nanospheres under an external field still possessed high magnetic responses. They could be easily separated from the solution within 10 s with a magnet and readily re-dispersed with a slight shake. The results revealed that the particles exhibited a magnetic response, as well and a re-disperse property, which suggested their potential application as a magnetic adsorbent. It could be concluded that all of the synthesized magnetic mesoporous nanoparticles had a superparamagnetic property. The superparamagnetic property of the prepared magnetic material could be very important for its applications because the particles could be easily removed by applying an external magnetic field after removing the metal ions in the aqueous solution, making them recyclable.

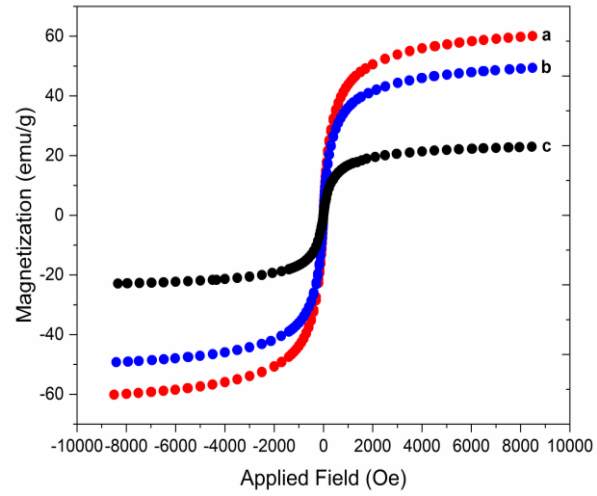

Fig. 6. Magnetic hysteresis loops of a: M-NPs, b: SCM-NPs, and c: IM-SCM NPs at room temperature using VSM.

Figure 7 shows the N_2 adsorption/desorption isotherms of the particles at 77 K. It also reveals a characteristic curve (type I) with a sharp capillary condensation step at a relative pressure from 0.2 to 0.4, which is characteristic of materials without pores. The corresponding pore size distribution of the sample was calculated by the desorption branches of the isotherms using the BJH method (Barrett-Joyner-Halenda). The pore size, BET surface area, and the total pore volume of the nanoparticles were 5.9 nm, 26 m^2/g, and 0.072 cm^3/g, respectively.

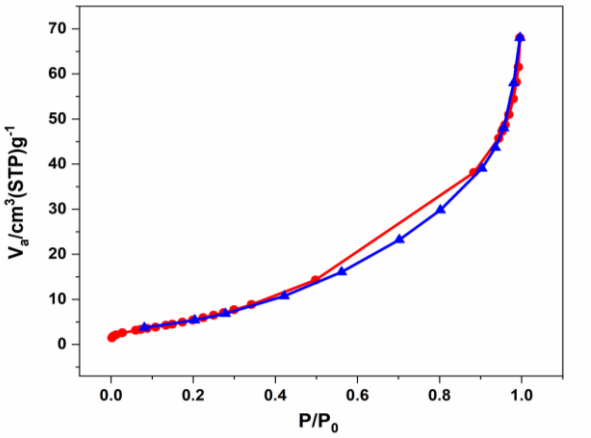

Fig. 7. N_2 adsorption/desorption isotherms of silica-coated magnetic nanoparticles.

3.2. The effect of pH on the extraction

The pH values of the samples were varied from 2 to 9 (using 1 M solutions of either nitric acid or sodium hydroxide) while performing the extraction experiments to evaluate the effects of pH on the extraction yield; the results were recorded (Figure 8). Based on the results, both ions were efficiently extracted using the IM-SCM NPs within a pH window of 5 to 9. It was probably due to the changes in the charges of the surface groups present on the adsorbent (e.g., -N and -OH). These are protonated at lower pH values, which form a more positive surface charge that repels the target cations. By increasing the pH of the solutions, the functional groups are gradually de-protonated; this increases the negative charges of the sites, which increases the tendency to electro-statically adsorb the Ag^+ and Cu^{2+} species. It must be mentioned that at low initial pH values, the influence of adsorption is the only effect responsible for reducing the heavy metal ions in the solution. However, at higher pH values (above 6.5 or 7), both the adsorption and aqueous metal hydroxide formation may become significant mechanisms in the metal removal process.

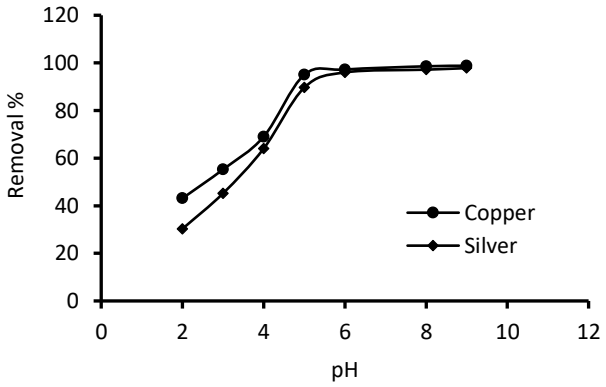

Fig. 8. Effect of pH on the removal efficiency of Ag^+ and Cu^{2+} ions.

3.3. Optimization of the amount of IM-SCM NPs

The optimal amount of IM-SCM NPs required for extracting the Ag+ and Cu2+ ions was investigated by performing different experiments in which the amount of the adsorbent was increased in the range of 10-30 mg into a 25 mL solution of 3 mg/L ions at a pH = 6. The results are presented in Figure 9. Based on these results, the removal efficiency first increased with the increase in the amount of the adsorbent because higher numbers of adsorption sites were available, but this reached an almost constant value. In light of the results, the remaining experiments were performed using 20 mg of IM-SCM NPs.

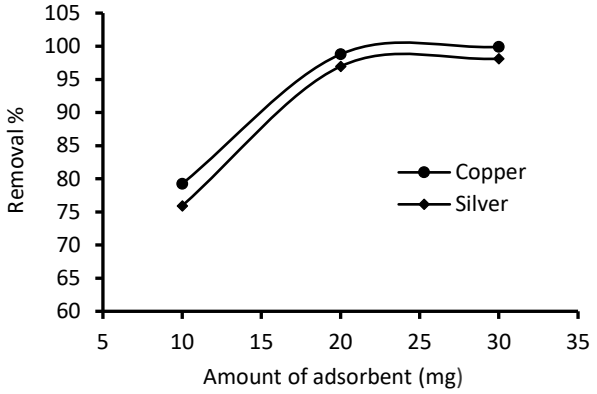

Fig. 9. Effect of the amount of adsorbent on the percentage of removal of Ag^+ and Cu^{2+} ions.

3.4. Optimizing the extraction time

A series of solutions containing 3 mg/L of Ag^+ and Cu^{2+} were used in these experiments and based on the results (Figure 10), the overall adsorption process had three phases, namely an initial rapid uptake phase, a slow uptake phase, and an equilibrium phase. In the first stage, due to the availability of a large number of vacant sites, strong concentration gradients were formed between the Ag^+ and Cu^{2+} concentrations in the solution and those in the adsorbent surface, which naturally led to the maximum sorption rate. In the next phase, the concentration gradient and the availability of adsorption sites were reduced, and hence, the adsorption rates decreased and finally reached equilibria. Based on the results, the best results were achieved after stirring the reaction mixture for 30 min or more, which was hence chosen as the optimal extraction time.

3.5. Effect of adsorbent modification

The effect of the modification of the MNPs on the removal of the target ions was evaluated using 20 mg of both SCM NPs and IM-SCM NPS in 25 mL of 3 mg/L of each ion. The resulting mixtures were gently shaken at ambient temperature for 30 min. The removal efficiency of Ag^+ and Cu^{2+} was relatively low (64% for Ag^+ and 82% for Cu^{2+}) in the case of the unmodified adsorbent, but increased (99% for Ag^+ and 100% for Cu^{2+}) in the case of the modified adsorbent, indicating that modification with the imine groups remarkably increased the removal of the target species.

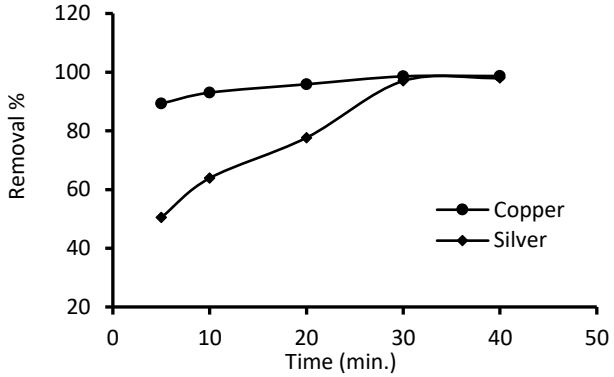

Fig. 10. Effect of contact time on the removal of Ag^+ and Cu^{2+} ions

Table 1. Removal of Ag^+ and Cu^{2+} ions from triple mixtures[a].

Divers ions	Amount taken (µg)	%Removal of Cu^{2+}	%Removal of Ag^+
Na^{2+}	250	100.0(0.9)[b]	---
Na^{2+}	150	---	100.0 (0.8)
Mg^{2+}	250	97.2(1.1)	---
Mg^{2+}	150	---	99.8 (0.9)
Cr^{3+}	250	95.3 (0.8)	---
Cr^{3+}	150	---	98.7 (1.0)
Co^{2+}	250	97.5 (1.0)	---
Co^{2+}	150	---	95.5 (1.1)
Pb^{2+}	250	97.8 (1.2)	---
Pb^{2+}	150	---	96.8 (0.9)
Ni^{2+}	250	100.0 (1.0)	---
Ni^{2+}	150	----	99.4 (0.6)
Zn^{2+}	250	99.2 (0.7)	----
Zn^{2+}	150	---	99.4 (1.0)
Cd^{2+}	250	98.2 (0.8)	---
Cd^{2+}	150	---	100.0 (0.9)
Mn^{2+}	250	97.5 (1.1)	---
Mn^{2+}	250	---	96.2 (1.2)

[a] Initial samples contained 75µg lead and cadmium ions in 25 ml water.

[b]Values in parentheses are RSDs based on three replicate analysis.

3.6. Removal of Ag^+ and Cu^{2+} ions in triple mixtures

To investigate the removal of Ag^+ and Cu^{2+}ions from aqueous solutions of different metal ions, 25 mL of solutions of 3 mg/L Ag^+ and Cu^{2+} as well as different amounts of other cations were prepared and subjected to adsorption experiments. In Table 1, the highest level of the third ion concentration, which do not indicate serious interference effects, is reported. According to these results, up to an acceptable level of the concentration of the third ionic species, Ag^+ and Cu^{2+}ions were fully removed by the adsorbents, and there was no serious interference-effect.

3.7. Adsorption isotherms

Establishing the best adsorption isotherm is important in optimizing the use of IM-SCM NPs. The parameters corresponding to each isotherm were determined through

linear regression analyses, and the square of the correlation coefficients (R^2) was also determined. The obtained isotherm values in Table 2 indicate that in the case of all the metal ions, the Langmuir isotherm model describes the isotherm data with respective correlation coefficients (R^2) of 0.990 and 0.992 for Ag^+ and Cu^{2+}; this indicates that the Ag^+ and Cu^{2+} ions form a homogeneous monolayer on the IM-SCM NPs. Based on the Langmuir analyses, the maximum adsorption capacities were 270 and 256 mg/g of IM-SCM of Ag^+ and Cu^{2+}, respectively.

Table 2. Values of isotherm constant for sorption of Ag^+ and Cu^{2+} ions.

Isotherm	Parameters	Ag^+	Cu^+
Langmuir	q_m(mg/g)	270.3	256.4
	K_L(L/mg)	0.011	0.008
	R^2	0.990	0.992
Freundlich	1/n	0.424	0.446
	K_f(mg/g)	17.03	12.99
	R^2	0.834	0.872
Temkin	B_1	59.44	56.17
	K_T(L/g)	0.104	0.079
	R^2	0.892	0.934

3.8. Desorption and reuse evaluating

Various experiments were performed to specify the proper volumes of nitric acid for recovering the adsorbed Ag^+ and Cu^{2+} ions from the IM-SCM NPs using different volumes of the acid. Based on the observations, 20 mL of the 3.0 mol/L nitric acid solution can lead to the quantitative elution of Ag^+ and Cu^{2+} from the adsorbent. Further tests were performed to assess the regeneration capacity of the adsorbents through repeated testing using the same samples of IM-SCM NPS; it was found that the recovery efficiency of IM-SCM NPs was reduced only 7% and 2% for Ag^+ and Cu^{2+}, respectively, after four use/regeneration cycles.

3.9. Removing Ag^+ and Cu^{2+} from wastewater

The application of the adsorbent in real samples was evaluated using different wastewater from pharmaceutical and battery factories. The wastewater samples were filtered using a 0.45-µm pore size membrane filter to remove suspended particulate matter, followed by a pH adjustment of about 6. Then, 20 mg of adsorbent was added to 25 mL of the wastewater sample and stirred for 30 min. The initial and residual concentrations of Ag^+ and Cu^{2+} in the samples were analyzed through the standard addition method because of the matrix effect. The results (Table 3) revealed that the adsorbent could be successfully used for removing the target ions from the wastewater samples with very good efficiency.

Table 3. Removal of Ag^+ and Cu^{2+} ions from wastewater samples.

Samples	Concentration of Ag^+(mg/L)	%Removal of Ag^+	Concentration of Cu^{2+}(mg/L)	%Removal of Cu^{2+}
Battery wastewater	0.29	91.3	0.16	85.4
Pharmaceutical wastewater	0.45	93.5	0.36	91.4

3.10. The effectiveness of the method vs. that of other reports

A comparison of the maximum capacity and optimal contact time of the adsorbent with those reported in previous works are presented in Table 4. The results clearly reveal that IM-SCM NPs are superior to all those used in former reports in terms of adsorption capacity [2,11,29-32] and to some in terms of contact time [29-31].

Table 4. Comparison of the proposed adsorbent with those previously reported.

Adsorbent	Maximum capacity (mg/g)	Contact time	Removed ions	Ref.
Magnetically modified MCM-41/piperazine	208.3	10 min.	Cu^{2+}	[2]
Guanidine functionalized SBA-15	57.0	10 min.	Cu^{2+}	[11]
ZnO/Granular Activated Carbon	16.6	3 days	Cu^{2+}	[29]
Waste coffee grounds	49.5	60 min.	Ag^+	[30]
Chitosan/montmorillonite	43.5	150 min.	Ag^+	[31]
Fe_3O_4-decorated and silica-coated graphene oxide modified with a polypyrrole-polythiophene copolymer	49	6.3 min.	Ag^+	[32]
silica-coated magnetic nanoparticles modified with imine	270 256	30 min. 30 min.	Ag^+ Cu^{2+}	This work

4. Conclusions

The main goal of the study was to develop a simple, rapid, and efficient adsorbent for simultaneous removing Ag^+ and Cu^{2+} ions from water and wastewater samples. To this end, imine-functionalized silica-coated Fe_3O_4 magnetic nanoparticles were prepared and used as a novel adsorbent for Ag^+ and Cu^{2+} removal. The imine-functionalized adsorbent was found to be an efficient tool for improving the efficiency of the silica-coated magnetite nanoparticles. In a solution of 25 mL with 3 mg/L of Ag^+ and Cu^{2+} ions, these ions were effectively removed from the solutions at a pH >5 after 30 min of stirring by using 20 mg of the IM-SCM NPS. The isotherm studies proved that the experimental data fit the Langmuir model better than the Freundlich and Temkin models. The highest adsorption capacity was respectively 270 and 256 mg of Ag^+ and Cu^{2+} ions per g IM-SCM NPS. The advantages of this adsorbent include a very short adsorption time, simple separation process, high adsorption capacity, and well-ordered pore distribution, which favor the homogeneity and reproducibility on the ion adsorption. Also, the regeneration and reuse capability of the adsorbent, as well as the need for a lesser amount, makes its application economically feasible.

Acknowledgment

The author thanks the Islamic Azad University of Yadegar-e-Imam Khomeini (RAH) Shahre-Rey branch Research Council for their support of this work.

References

[1] Dubey, S., Banerjee, S., Upadhyay, S. N., Sharma, Y. C. (2017). Application of common nano-materials for removal of selected metallic species from water and wastewaters: A critical review. *Journal of molecular liquids, 240*, 656-677.

[2] Kanani, N., Bayat, M., Shemirani, F., Ghasemi, J. B., Bahrami. Z., Badiei, A. (2018). Synthesis of magnetically modified mesoporous nanoparticles and their application in simultaneous determination of Pb(II), Cd(II) and Cu(II). *Research on chemical intermed*iates, *44(3),* 1688-1709.

[3] Vojoudi, H., Badiei, A., Banaei, A., Bahar, S., Karimi, S., Ziarani, G. M., Ganjali, M. R. (2017). Extraction of gold, palladium and silver ions using organically modified silica-coated magnetic nanoparticles and silica gel as a sorbent. *Microchimica acta, 184(10),* 3859-3866.

[4] Vojoudi, H., Badiei, A., Amiri, A., Banaei, A., Mohammadi Ziarani, G., Schenk-Joß, K. (2018). Efficient device for the benign removal of organic pollutants from aqueous solutions using modified mesoporous magnetite nanostructures. *Journal of physics and chemistry of solids*, *113*, 210-219.

[5] Poursaberi, T., Ghanbarnejad, H., Akbar, V. (2012). Selective magnetic removal of Pb(II) from aqueous solution by porphyrin linked-magnetic nanoparticles, *Journal of nanostructures, 2*(4), 417-426.

[6] Kakaei, A., Kazemeini, M. (2016). Removal of Cd (II) in water samples using modified magnetic Iron oxide nanoparticle. *Iranian journal of toxicol*ogy, *10*, 9-14.

[7] Lam, K. F., Yeung, K. L., Mckay, J. (2007). Selective mesoporous adsorbents for $Cr_2O_7^{2-}$ and Cu^{2+} separation. *Microporous and mesoporous mater*ials, 100, 191-201.

[8] Hajiaghababaei, L., Badaei, A., Ganjali, M. R., Heydari, S., Khaniani, Y., Mohammadi Ziarani, G. (2011). Highly efficient removal and preconcentration of lead and cadmium cations from water and wastewater samples using ethylenediamine functionalized SBA-15. *Desalination*, *266(1-3),* 182-187.

[9] Hajiaghababaei, L., Ghasemi, B., Badiei, A., Goldooz, H., Ganjali, M. R., Mohammadi Ziarani, G. (2012). Aminobenzenesulfonamide functionalized SBA-15 nanoporous molecular sieve: A new and promising adsorbent for preconcentration of lead and copper ions. *Journal of environmental sci*ence, *24(7),* 1347-1354.

[10] Hajiaghababaei, L., Badiei, A., Shojaan, M., Ganjali, M. R., Mohammadi Ziarani, G., Zarabadi-Poor, P. (2012). A novel method for the simple and simultaneous preconcentration of Pb^{2+}, Cu^{2+} and Zn^{2+} ions with aid of diethylenetriamine functionalized SBA-15 nanoporous silica compound. *International journal of environmental analytical chemistry*, *92(12),* 1352-1364.

[11] Hajiaghababaei, L., Tajmiri, T., Badiei, A., Ganjali, M. R., Khaniani, Y., Mohammadi Ziarani, G. (2013). Heavy metals determination in water and food samples after preconcentration by a new nanoporous adsorbent. *Food chem*istry, *141(3),* 1916-1922.

[12] Ganjali, M. R., Hajiaghababaei, L., Badaei, A., Saberyan, K., Salavati-Niasari, M., Mohammadi Ziarani, G., Behbahani, S. M. R. (2006). A novel method for fast enrichment and monitoring of hexavalent and trivalent chromium at the ppt level with modified silica MCM-41 and its determination by inductively coupled plasma optical emission spectrometry. *Quimica nova*, *29(3),* 440-443.

[13] Ganjali, M. R., Hajiaghababaei, L., Norouzi, P., Pourjavid, M. R., Badaei, A., Saberyan, K., Ghannadimaragheh, M., Salavati-Niasari, M., Ziarani, G. M. (2005). Novel method for the fast separation and purification of molybdenum(VI) from fission products of uranium with aminofunctionalized Mesoporous molecular sieves (AMMS) modified by dicyclohexyl-18-crown-6 and S-N tetradentate Schiff's base. *Analytical letter, 38*(11), 1813-1821.

[14] Ganjali, M. R., Hajiaghababaei, L., Badaei, A., Ziarani G. M., Tarlani, A. (2004). Novel method for fast preconcentration and monitoring of a ppt level of lead

and copper with a modified hexagonal mesoporous silica compound and inductively coupled plasma atomic emission spectrometry. *Analytical science*, *20*, 725-729.

[15] Lim, M. H., Stein, A. (1999). Comparative studies of grafting and direct syntheses of inorganic−organic Hybrid Mesoporous materials. *Chemistry of materials*, *11*(11), 3285-3295.

[16] Ho, K. Y., Mckay, G., Yeung, K. L. (2003). Selective adsorbents from ordered mesoporous silica. *langmuir*, *19(7)*, 3019-3024.

[17] Hajiaghababaei, L., Abozari, S., Badiei, A., Zarabadi Poor, P., Dehghan Abkenar, S., Ganjali, M. R., Mohammadi Ziarani, G. (2017). Amino ethyl-functionalized SBA-15: A promising adsorbent for anionic and cationic dyes removal. *Iranian journal of chemistry and chemical engineering (IJCCE)*, *36*(1), 97-108.

[18] Habibi, S., Hajiaghababaei, L., Badiei, A., Yadavi, M., Abkenar, S. D., Ganjali, M. R., Ziarani, G. M. (2017). Removal of reactive black 5 from water using carboxylic acid-grafted SBA-15 nanorods. *Desalination and water treatment*, *95*, 333-341.

[19] Ju, Y. H., Webb, O. F., Dai, S., Lin, J. S., Barnes, C. E. (2000). Synthesis and characterization of ordered mesoporous anion-exchange inorganic/organic hybrid resins for radionuclide separation. *Industrial and engineering chemistry research*, *39*(2), 550-553.

[20] Lee, B., Bao, L. L., Im, H. J., Dai, S., Hagaman, E. W., Lin, J. S. (2003). Synthesis and characterization of organic–inorganic hybrid mesoporous anion-exchange resins for perrhenate (ReO_4-) Anion adsorption. *Langmuir*, *19*(10), 4246-4252.

[21] Fryxell, G. E., Liu, J., Hauser, T. A., Nie, Z., Ferris, K. F., Mattigod, S., Hallen, R. T. (1999). Design and synthesis of selective mesoporous anion traps. *Chemistry of materials*, *11*(8), 2148-2154.

[22] Vojoudi, H., Badiei, A., Amiri, A., Banaei, A., Ziarani, G. M., & Schenk-Joß, K. (2018). Pre-concentration of Zn (II) ions from aqueous solutions using meso-porous pyridine-enrobed magnetite nanostructures. *Food chemistry*, *257*, 189-195.

[23] Vojoudi, H., Badiei, A., Bahar, S., Ziarani, G. M., Faridbod, F., Ganjali, M. R. (2017). A new nano-sorbent for fast and efficient removal of heavy metals from aqueous solutions based on modification of magnetic mesoporous silica nanospheres. *Journal of magnetism and magnetic materials*, *441*, 193-203

[24] Saad, A. H. A., Azzam, A. M., El-Wakeel, S. T., Mostafa, B. B., El-latif, M. B. A. (2018). Removal of toxic metal ions from wastewater using ZnO@ Chitosan core-shell nanocomposite. *Environmental nanotechnology, monitoring and management*, *9*, 67-75.

[25] Wang, X., Guo, Y., Yang, L., Han, M., Zhao, J., Cheng, X. (2012). Nanomaterials as sorbents to remove heavy metal ions in wastewater treatment. *Journal of environmental and analytical toxicology, 2*(7), 154.

[26] Langmuir, I. (1918). The adsorption of gases on plane surfaces of glass, mica and platinum. *Journal of the American chemical society*, *40*(9), 1361-1403.

[27] Freundlich, H. M. F. (1906). Over the adsorption in solution. *Journal of physical chem*istry, *57*, 385-470.

[28] Temkin, M. I. (1940). Kinetics of ammonia synthesis on promoted iron catalysts. *Acta physiochim. URSS*, *12*, 327-356.

[29] Kikuchi, Y., Qian, Q., Machida, M., Tatsumoto, H. (2006). Effect of ZnO loading to activated carbon on Pb (II) adsorption from aqueous solution. *Carbon*, *44*(2), 195-202.

[30] Jeon, C. (2017). Adsorption of silver ions from industrial wastewater using waste coffee grounds. *Korean journal of chemical engineering*, *34*(2), 384-391.

[31] Jintakosol, T., Nitayaphat, W. (2016). Adsorption of silver (I) from aqueous solution using chitosan/montmorillonite composite beads. *Materials research*, *19*(5), 1114-1121.

[32] Jalilian, N., Ebrahimzadeh, H., Asgharinezhad, A. A., Molaei, K. (2017). Extraction and determination of trace amounts of gold (III), palladium (II), platinum (II) and silver (I) with the aid of a magnetic nanosorbent made from Fe_3O_4-decorated and silica-coated graphene oxide modified with a polypyrrole-polythiophene copolymer. *Microchimica acta*, *184*(7), 2191-2200.